Natural Rubber/Multiwalled Carbon Nanotube Composites Developed with a Combined Self-Assembly and Latex Compounding Technique

Zheng Peng,[1] Chunfang Feng,[1,2] Yongyue Luo,[1] Yongzhen Li,[1] Zhifeng Yi,[1,2] L. X. Kong[2]

[1]*Chinese Agricultural Ministry Key Laboratory of Tropical Crop Product Processing, Agricultural Product Processing Research Institute, Chinese Academy of Tropical Agricultural Sciences, Zhanjiang 524001, China*
[2]*Centre for Material and Fibre Innovation, Institute for Technology Research Innovation, Deakin University, Geelong Vic 3217, Australia*

Received 17 November 2009; accepted 3 October 2010
DOI 10.1002/app.36389
Published online in Wiley Online Library (wileyonlinelibrary.com).

ABSTRACT: Carbon nanotubes (CNTs), with their high aspect ratio and exceptionally high mechanical properties, are excellent fillers for composite reinforcement if they are uniformly dispersed without aggregation. Combining the latex compounding and self-assembly techniques, we prepared a novel natural rubber (NR)/multiwalled carbon nanotube (MWCNT) composite. Before self-assembly, the MWCNTs were treated with mixed acid to ensure that the MWCNTs were negatively charged under an alkaline environment. The structure of the MWCNTs was tested with Fourier transform infrared spectroscopy. The properties of composites with different MWCNT loadings were characterized with transmission electron microscopy, scanning electron microscopy, thermogravimetric analysis, and tensile testing. The results indicate that the MWCNTs were homogeneously distributed throughout the NR matrix as single tubes and had good interfacial adhesion with the NR phase when the MWCNT loading was less than 3 wt %. In particular, the addition of the MWCNT led to a remarkable reinforcement in the tensile strength, with a peak value of 31.4 MPa for an MWCNT content of 2 wt %, compared to the pure prevulcanized NR (tensile strength = 21.9 MPa). The nanocomposites reinforced with MWCNTs should have wide applications because of the notable improvement in these important properties. © 2012 Wiley Periodicals, Inc. J Appl Polym Sci 000: 000–000, 2012

Key words: composite; latex compounding; multi-walled carbon nano-tube; natural rubber; self-assembly

INTRODUCTION

Nanoparticles are widely used in many polymers, endowing nanocomposites with unique mechanical, thermal, optical, and electromagnetic properties, because of their special surface, size, and quantum effects.[1–3] Carbon nanotubes (CNTs) are constructed with a high length-to-diameter ratio, which is significantly larger than that of any other material. These cylindrical carbon molecules have novel properties, including an extraordinarily high strength and good electrical and thermal conductivities; these properties make them potentially useful in many applications.[4,5] However, CNTs without surface modification are not easily evenly dispersed in polymer materials. For single-walled CNTs, the surface functionalization of CNTs mainly includes covalent and noncovalent modification (Fig. 1).[6] Acid oxidation is one of the most effective modification methods, if the vent gas can be disposed well.

Natural rubber (NR), as one of the most important biosynthesized polymers with excellent chemical and physical properties, is playing a very important role in a number of industries and has a broad range of applications.[7,8] The sol–gel process, intercalation, and physical blending are the main conventional methods used to synthesize NR/inorganic nanocomposites.[9] However, there are some weaknesses in these methods. For example, NR/inorganic nanocomposites prepared with the sol–gel method possess an awful reliability and repeatability.[10] The intercalation process is only suitable for clay-based nanocomposites and not for NR/inorganic composites with higher specific surfaces, despite the fact

Correspondence to: Z. Peng (zhengpeng8@yahoo.com) or L. X. Kong (lingxue.kong@deakin.edu.au).

Contract grant sponsor: Ministry of Science and Technology R & D Research Institutes; contract grant number: 2008EG134285.
Contract grant sponsor: 973 Program Special Fund; contract grant number: 2010CB635109.

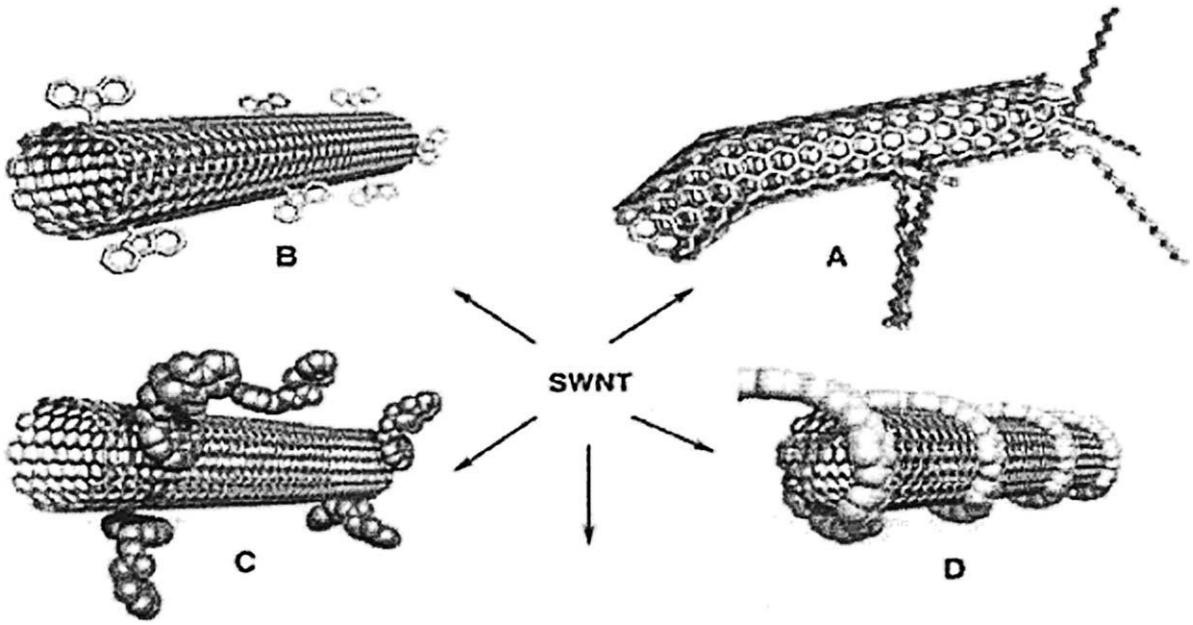

Figure 1 Surface-functionalized single-walled CNTs (SWNTs): (A) defect-group functionalization, (B) covalent sidewall functionalization, (C) noncovalent exohedral functionalization with surfactants, and (D) noncovalent exohedral functionalization with polymers.[6]

that inorganic nanoparticles of high specific surfaces have a better enhancement effect on the polymers.[11] As to physical blending, inorganic nanoparticles tend to self-aggregate during the assembling process because their high surface potential energy leads to strong particle–particle interaction.[12] Consequently, to further extend NR applications, it is critical to explore a new approach to enhance the properties of NR.

In this article, a novel NR/multiwalled carbon nanotube (MWCNT) composite was prepared by the combination of self-assembly and latex-compounding techniques; this has not been previously reported in the rubber composite research. In previous work, a process was developed that incorporates the latex compounding and self-assembly techniques to prepare poly(vinyl alcohol)/silica and rubber/silica nanocomposites.[13,14] The results show that the chemical and physical properties of the nanocomposites, compared to those of the polymer host, were significantly improved. In this work, this self-assembly process was extended to prepare NR/MWCNT composites and to investigate the self-assembly mechanism between MWCNTs and NR particles. An in-depth study of the relationship between the morphology and properties of the composites was also undertaken.

EXPERIMENTAL

Materials

NR latex with a total solid content of 60% was purchased from Qianjin State Rubber Farm (Zhanjiang, China) and was prevulcanized. MWCNTs (average diameter = 10–30 nm, average length = 5–15 μm, purity ≥ 95%) were obtained from Tannamigang Co. (Shenzhen, China). The surfactant used for the dispersal of MWCNTs was sodium dodecyl sulfate (SDS; 90%, Merck Chemical Co. Poly(diallyldimethylammonium chloride) (PDDA; molecular weight ≈ 100,000–200,000, 20 wt % in water) was bought from Sigma-Aldrich (St. Louis, MO). All of the inorganic acids were analytical-reagent grade.

Preparation of the acid-treated multiwalled carbon nanotubes (a-MWCNTs)

A typical procedure was as follows: a certain amount of pristine multiwalled carbon nanotubes (p-MWCNTs) was added to a 250-mL flask charged with H_2SO_4–HNO_3 (3 : 1 v/v) solution.[15] The

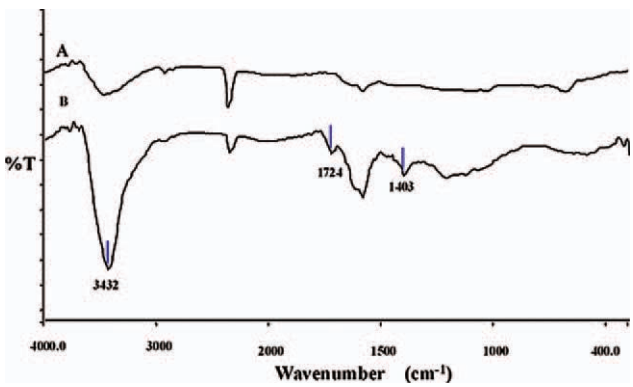

Figure 2 Infrared spectra of (A) p-MWCNTs and (B) a-MWCNTs. [Color figure can be viewed in the online issue, which is available at wileyonlinelibrary.com.]

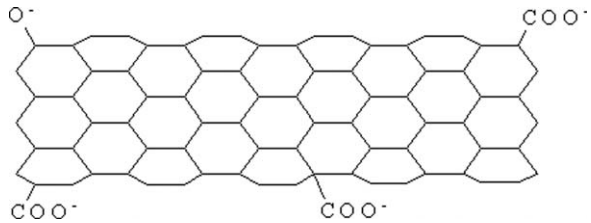

Scheme 1 Structure of the acid-oxidized MWCNTs at a pH value of 10.

mixture was heated for 1.5 h and then diluted in a 1000-mL beaker with 800 mL of deionized water. After it was cooled to room temperature, the mixture was filtered through a 200-nm pore diameter membrane and washed with deionized water until it was neutral. The resulting black solid was then dried in a vacuum freeze dryer for 48 h.

Preparation of positively charged MWCNTs

MWCNTs treated with SDS (MWCNT/SDS = 2/1 w/w) were dispersed in 100 mL of water and were treated with an ultrasonic vibrator for 0.5 h.[16] Their pH value was then adjusted to 10 with 0.2*M* KOH to obtain a negatively charged MWCNT dispersion. A fixed amount of positively charged PDDA solution (0.5 wt %, pH 10) was dropped into the MWCNT dispersion (MWCNT/PDDA = 10 : 1 w/w) with magnetic stirring for 0.5 h.

Preparation of the NR/MWCNT composites

NR latex was prevulcanized by the addition of a curing system for 2 h at 60°C, and finally, the total solid content was 50%. MWCNTs modified by a PDDA aqueous dispersion (MWCNT–PDDA) were dropped into negatively charged NR latex (prevulcanized, pH 10) with different mixture rates (NR/MWCNT = 99.5/0.5, 99/1.0, 98/2.0, 97/3.0, and 95/5.0 w/w) with gentle magnetic stirring at room temperature for 24 h. Finally, the mixture was cast onto glass plates and dried at 50°C to obtain the NR/MWCNT composite films. A reference sample was prepared with the same process with MWCNTs that were not treated with acid, SDS, and PDDA.

Characterization

Surface functional groups of the MWCNTs after oxidation were investigated on a PerkinElmer Spectra GX-I Fourier transform infrared (FTIR) spectroscope (Fremont, CA) with a resolution of 4 cm^{-1} in the transmission mode. The ζ potential analysis of the MWCNTs and NR was performed with a Nano-ZS MPT ζ-size analyzer (Malvern, United Kingdom). The NR/MWCNT dispersion was dragged up by a copper network and then observed with transmission electron microscopy (TEM; JEOL, Peabody, MA) at an accelerating voltage of 100 kV. Scanning electron micrographs of the nanocomposites were taken with a Philips XL30-EDAX instrument (Philips, Eindhoven, The Netherlands) at an acceleration voltage of 10 kV. We obtained the fracture surface by splitting bulk samples being quenched in liquid nitrogen. A PerkinElmer TGA-7 thermogravimetric (TG) analyzer was used for thermal and thermooxidative decomposition measurements. In nitrogen, the measurement of the films (ca. 10 mg) was carried out from 100 to 600°C at a heating rate of 20°C/min. Tensile tests were conducted on an Instron Series IX automated materials testing system (Acton, MA) at room temperature with a crosshead

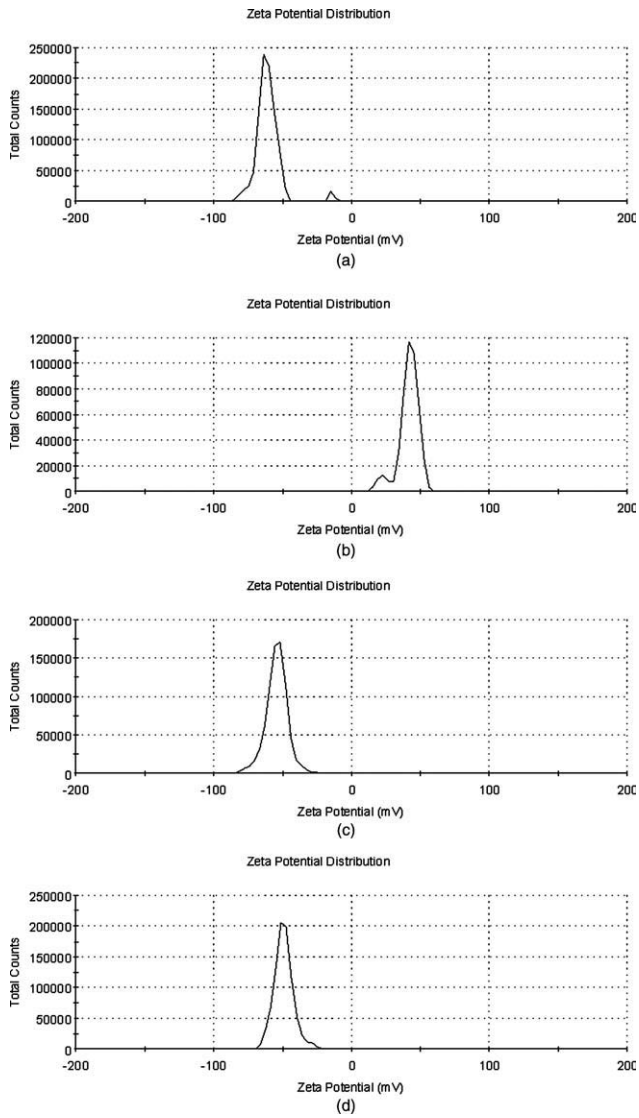

Figure 3 ζ potential distribution of the MWCNTs, NR, and composites: (a) MWCNTs aqueous solution (pH 10, −60.9 mV), (b) MWCNT–PDDA aqueous solution (pH 10, 41.5 mV), (c) pure prevulcanized NRL (pH 10, −54.4 mV), and (d) NR/MWCNT–PDDA (MWCNT–PDDA/NR = 2/100, −49.2 mV).

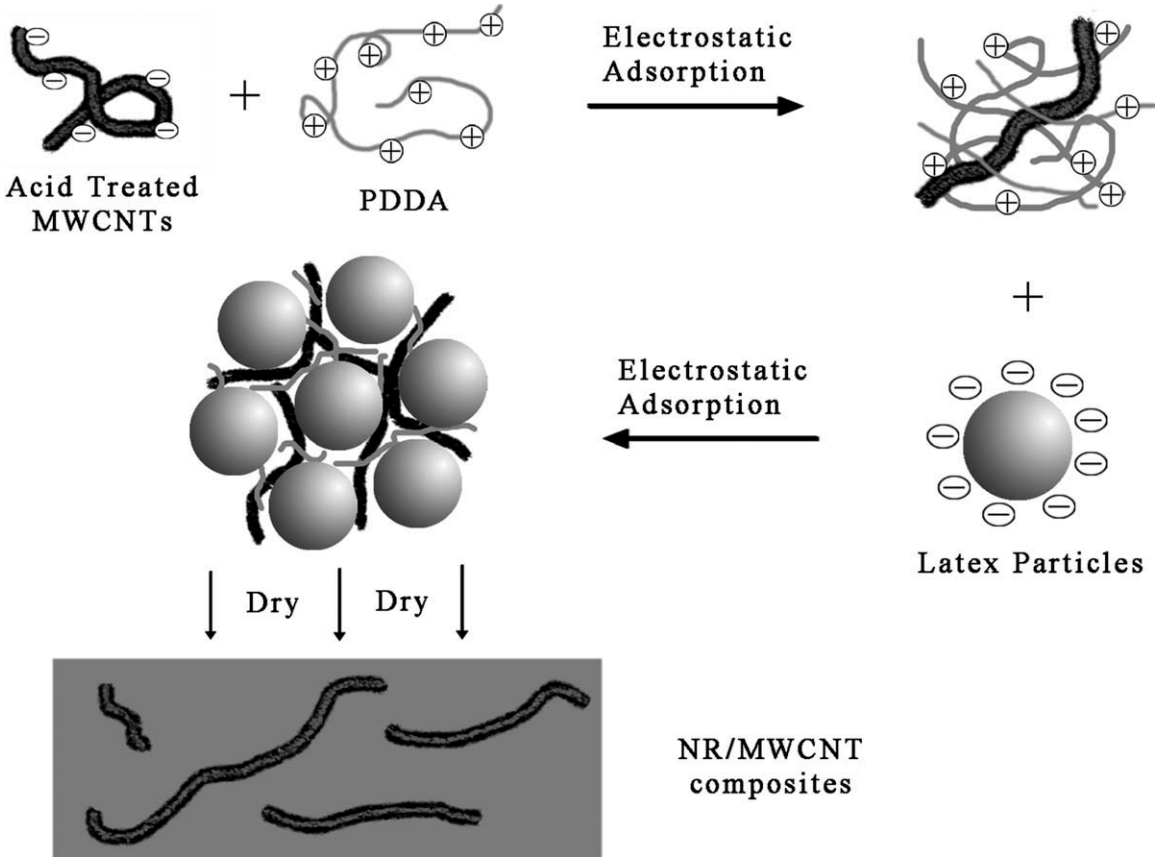

Figure 4 Schematic of the self-assembly process.

speed of 500 mm/min; the sample length between the jaws was 25 mm, and the sample width was 4 mm.

RESULTS AND DISCUSSION

FTIR analysis

There were absorption bands at 3432 cm^{-1} from the FTIR spectra of both the p-MWCNTs [Fig. 2(A)] and a-MWCNTs [Fig. 2(B)]; these were assigned to the stretching vibrations of hydroxyl groups (—OH). This might have been caused by the residual water absorbed on the surface of the MWCNTs. Moreover, the absorption band centered at 3432 cm^{-1} for the a-MWCNTs [Fig. 2(B)] was stronger than in the spectra of the p-MWCNTs; therefore, a certain number of —OH groups were introduced onto the surface of the MWCNTs. Compared with the p-MWCNTs, new bands appeared at 1724 and 1403 cm^{-1} in the spectra of the a-MWCNTs; these were assigned to the stretching vibrations of carbonyl groups (—C=O) and carboxylic acid groups ($—COO^-$), respectively. So, it was proven that —COOH groups were successfully introduced onto the surface of the MWCNTs. With these hydrophilic groups, the a-MWCNTs disperses better in water than the p-MWCNTs.[17]

Self-assembly mechanism between the MWCNTs and NR particles

In the current work, self-assembly technique first introduced by Decher et al.[18] was employed to prepare NR/MWCNT composite. Interactions such as electrostatic attraction, hydrophobic interaction,[19] charge transfer interaction,[20] H bonding, coordination bonding,[21] and covalent bonding are the most widely used forces for self-assembly. In this study, electrostatic attraction was used as the driving force.

Because the p-MWCNTs were very stable and their surface was chemically inert and hydrophobic, it was hard to disperse them in NR latex, a water-based latex. Therefore, acid was used to treat the MWCNTs before the self-assembly process. The acid treatment successfully introduced carboxylic and hydroxyl groups onto the surface of the MWCNTs,

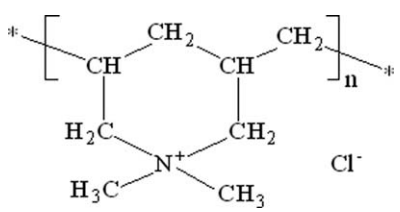

Scheme 2 Structure of PDDA at a pH value of 10.

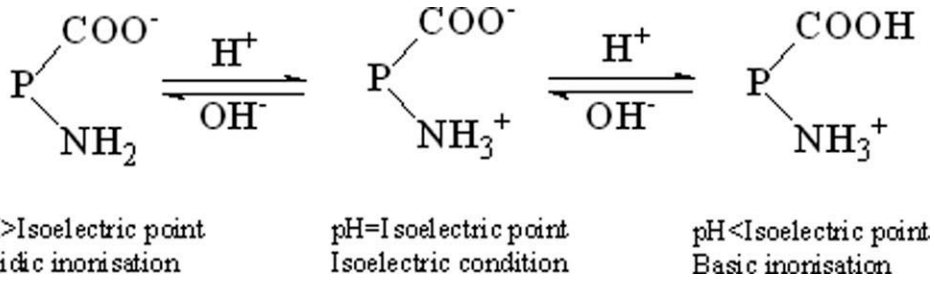

Scheme 3 Charged mechanism of the NR particle.

which greatly improved the water solubility of the CNTs and made it possible for the CNTs to be negatively charged at pH 10 (Scheme 1). After the acid treatment of the MWCNTs, the ζ potential of the a-MWCNT solution (pH 10) was −60.9 mV [Fig. 3(a)].

Generally speaking, the self-assembly process of the NR/MWCNT composites involved two steps (Fig. 4). In the first step, PDDA, a universally used self-assembly material, was positively charged at pH 10 (Scheme 2)[22–24] and was assembled onto the surface of negatively charged MWCNTs with electrostatic adsorption as a driving force. However, there were numerous differences in rigidity between the MWCNTs and PDDA, and the charge density of PDDA was significantly larger than that of the MWCNTs, so all of the former charges could not form short-distance ion pairs with the surface charges of the rigid MWCNTs. Therefore, the positive charge on PDDA could not completely be neutralized by the negative charge on the MWCNTs during the assembly, and the MWCNT–PDDA particles became positive and were ready for the second assembly with negatively charged NR particles. As shown in Figure 3(b), the ζ potential of the MWCNT–PDDA solution (pH 10) was 41.5 mV.

It was the high electrostatic energy barrier outside the MWCNTs that slowed down the self-aggregation of the MWCNTs. As protein particles, the NR particles contained carboxyl and amino functional groups. If the pH is higher than the isoelectric point of NR latex (4.5–5.0), such as the pH used in the experiment (pH 10), acidic ionization will occur, and NR particles will be negatively charged in the second step (Scheme 3).[14] As shown in Figure 3(c), the ζ potential of the pure prevulcanized latex (pH 10) was −54.4 mV.

Driven by electrostatic adsorption, MWCNT–PDDA was adsorbed onto the surface of the NR particles. Finally, the MWCNTs were uniformly dispersed in the NR matrix to form a nanocomposite. Because MWCNT–PDDA accounted for a small proportion in the composites [Fig. 3(d)], the ζ potential of the composite was negatively charged. The proportion of MWCNTs, PDDA, and latex was well

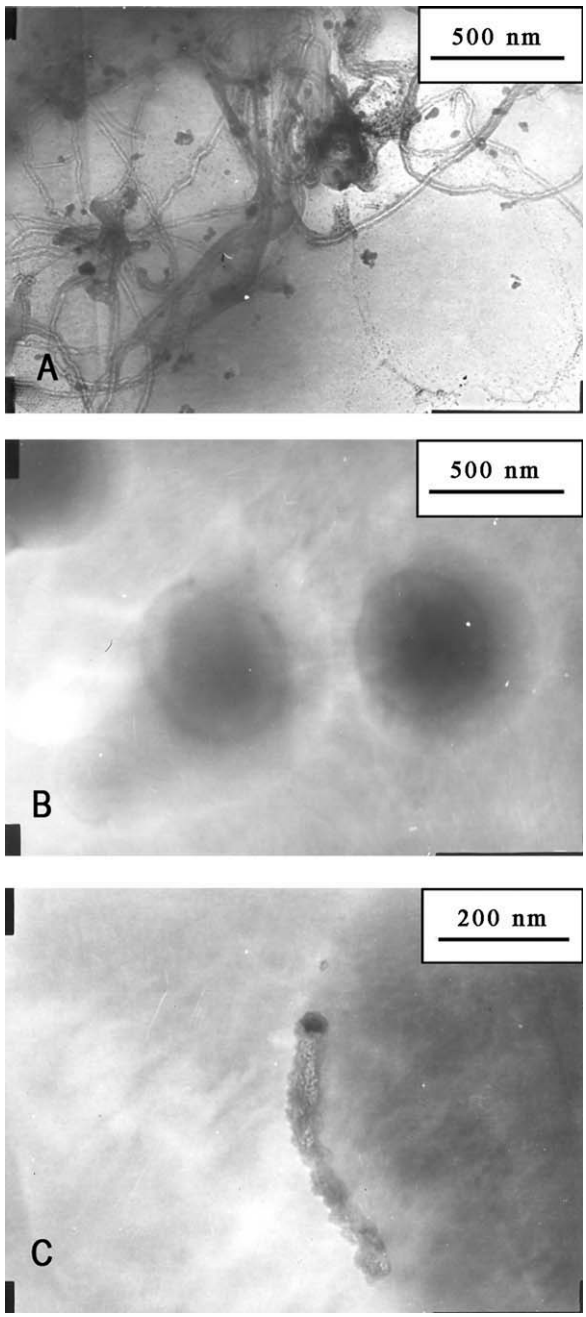

Figure 5 TEM micrographs of the NR/MWCNT composites: (A) p-MWCNT (1 wt %) dispersed in NRL, (B) MWCNT–PDDA assembled with NR particles, and (C) partly enlarged view of part B.

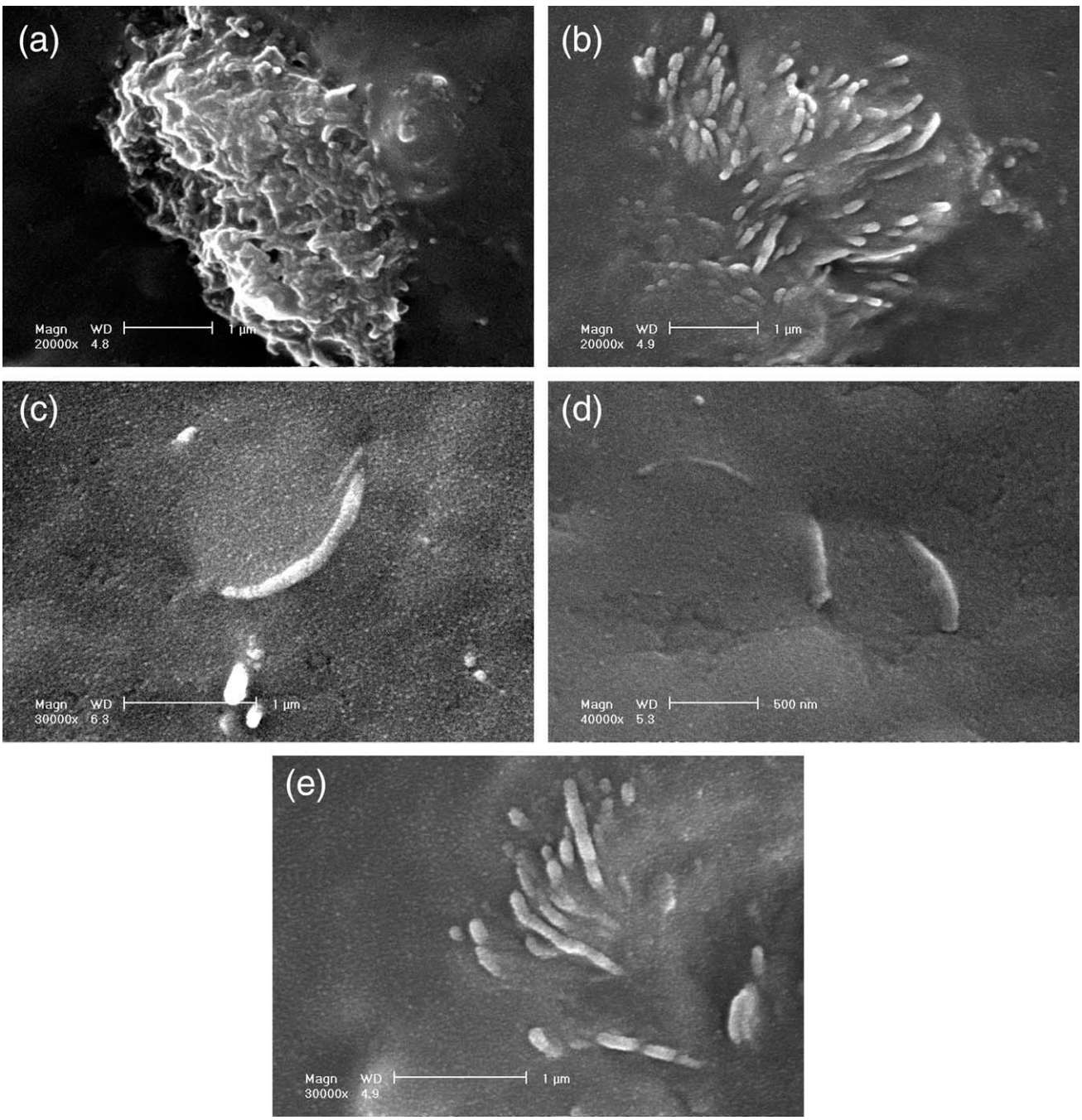

Figure 6 SEM micrographs of the NR/MWCNT composites: (A) p-MWCNT (1 wt %) dispersed in an NR matrix, (B) a-MWCNT (1 wt %) dispersed in an NR matrix, (C) MWCNT–PDDA (0.5 wt %) dispersed in an NR matrix, (D) MWCNT–PDDA (2 wt %) dispersed in an NR matrix, and (E) MWCNT–PDDA (5 wt %) dispersed in an NR matrix.

maintained for all experiments; no significant flocculation was observed.

Morphology of the NR/MWCNT composites

The interaction between fillers and polymers can directly affect the performance of a matrix, and it has rarely been reported that agglomerations of fillers can significantly increase the properties of composites as a good distribution of fillers is almost imperative for effective reinforcement.[25] Because it is hydrophobic, it is impossible for p-MWCNTs to be dispersed as individual CNTs in a high-viscosity polymer matrix.[26] The p-MWCNTs were in an aggregated and twisted form in the NR matrix [Fig. 5(A)].

However, MWCNT–PDDA prepared with the self-assembly technique was more intimate with the NR matrix [Fig. 5(B)] and could be individually attached to the NR particles like a little worm [Fig. 5(C)]. This led to a significant increase in the mechanical

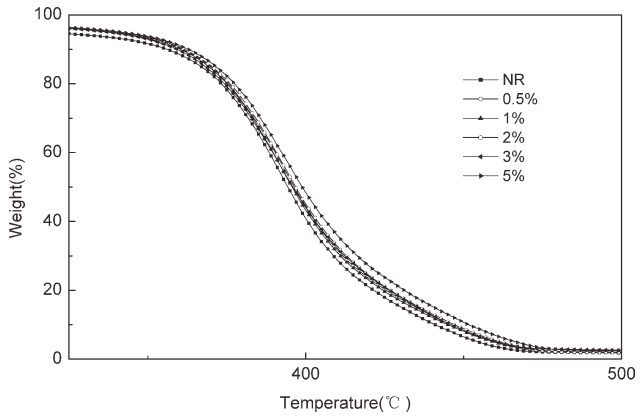

Figure 7 TG curves of the NR and NR/MWCNT composites in N_2.

properties[17] because of the favorable dispersion of the MWCNTs.

The morphology of the nanocomposites with different MWCNT loadings was also studied with scanning electron microscopy (SEM; Fig. 6), where the dark phase represented NR, and the light phase represented the MWCNTs. The p-MWCNTs aggregated in NR and were incompatible with NR, as demerit or incompact structures were clearly observed around the NR interface [Fig. 6(A)], whereas the a-MWCNTs, which were in a boscagelike form [Fig. 6(B)], were obviously dispersed in NR as a much improved individual phase compared to the clewlike structure of the p-MWCNTs. In addition, the interface between the PDDA-modified MWCNTs and NR seemed very smooth; this indicated that the severe self-aggregation or twisting of p-MWCNTs was greatly depressed, and the interfacial adhesion between the MWCNTs and NR was remarkably enhanced. This was in good agreement with TEM observation [Figs. 6(C–E)]. PDDA, used as a bridge, played a critical role in the preparation of the CNT nanocomposites to facilitate the incorporation of MWCNTs with the NR particles, to prevent the aggregation or twisting of the MWCNTs, and to enhance the interfacial adhesion between the MWCNTs and NR matrix.

However, a further increase in the MWCNT content had an unfavorable effect on its dispersion in the NR latex. When the MWCNT content was less than 3 wt %, almost all MWCNTs were homogeneously distributed throughout the NR matrix as individual CNTs [Fig. 6(C,D)], but the MWCNTs tended to aggregate when the MWCNT content was increased further [Fig. 6(E)]. The effect of the MWCNT dispersion in NR on the properties of nanocomposites will need to be examined further in the future.

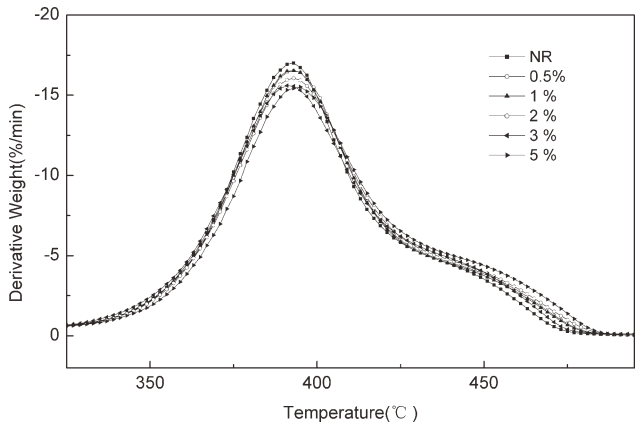

Figure 8 DTG curves of the NR and NR/MWCNT composites in N_2.

Thermal degradation of the NR/MWCNT composites

Figures 7 and 8 present the TG and derivative thermogravimetric (DTG) curves, respectively, of the NR and NR/MWCNT composites in nitrogen with a heating rate of 20°C/min. In this study, TG analysis provided information on the various degradation parameters and degradation kinetic factors. For both the NR and NR/MWCNT composites, there was only one turn in the TG curves and one corresponding weight loss peak in the DTG curves; this indicated that there was only one obvious decomposition step in the NR molecular chains, which was primarily initiated by thermal scission of the C—C chain bonds accompanied by a transfer of hydrogen at the site of scission.[27] The degradation curve of the NR/MWCNT composites with different amounts of fillers showed a slight shift to higher temperature.

The initial degradation temperature (T_0) and final degradation temperature (T_f) were calculated with a bitangent method from the TG curves, and the peak degradation temperature (T_p), the temperature at maximum degradation rate, was obtained from the DTG curves. The various degradation temperatures of the NR/MWCNT composites were slightly higher than those of the NR (Table I). During thermal decomposition, T_0, T_p, and T_f of the NR/MWCNT

TABLE I
Characteristic Temperatures of Thermal Decomposition for the Pure NR and NR/MWCNT Composites with Different MWCNT Contents

	Thermal decomposition			
Sample	T_0	T_p	T_f	ΔT
NR	361.5	389.0	418.1	56.6
0.5%	361.9	390.1	424.0	62.1
1.0%	363.2	390.8	425.9	62.7
2.0%	364.4	391.2	427.9	63.5
3.0%	366.2	392.5	428.0	61.8
5.0%	368.3	394.0	430.1	61.8

TABLE II
Mechanical Properties of the Pure NR and NR/MWCNT Composites

MWCNT loading (wt %)	0	0.5	1	2	3	5
Tensile strength (MPa)	21.9 (±0.6)	25.0 (±0.3)	30.0 (±1.3)	31.4 (±0.6)	28.7 (±1.3)	25.0 (±0.9)
Tensile modulus (MPa)						
300% elongation	0.89	1.02	1.30	1.35	1.52	1.31
500% elongation	1.32	1.72	2.30	2.63	3.05	2.53
700% elongation	4.76	5.74	8.89	9.06	9.55	7.57
Elongation at break (%)	945	940	962	908	883	854

composites with 5 wt % MWCNT loading increased by 6.8, 5, and 12°C, respectively, compared to those of the NR. As there was no chemical bond between the NR and MWCNT particles by a self-assembly process, it was easy for the NR and MWCNT particles to break down during heating, so the thermal stability of the NR composite was not remarkably improved by the addition of the MWCNTs.

A reason for the improvement in the aging resistance of the NR/MWCNT composites was that inorganic nanoparticles migrated to the surface of the composites at elevated temperatures because of their relatively low surface potential energy.[28] The addition of the MWCNTs enhanced the thermal-resistance properties because a strong polymeric–inorganic char was formed as a result of the nanoparticles' migration, and the role of nanoparticles in the thermal properties of nanocomposites is commonly attributed to the barrier model.

Tensile properties

The tensile strength, tensile modulus, and elongation at break values for the NR and NR/MWCNT composites filled with different MWNCT loadings are presented in Table II. Compared with NR, the addition of MWCNT–PDDA led to a remarkable increase in the tensile strength and tensile modulus. Generally, the higher the a-MWCNT loading was, the higher the tensile strength and the tensile modules were when the loading was less than 2%. The composite was the strongest when the MWCNT loading was between 1 and 2 wt % and increased by 8–9.5 MPa, a 50% increase compared to pure prevulcanized NR. This also represented a significant improvement in the tensile strength compared with nanocomposites reinforced with other fillers.[29] However, with further addition of MWCNTs, the tensile strength gradually decreased because of MWCNT aggregation; this was in agreement with the structural characteristics deduced from SEM observation.

Another subtle change in the elongation at break was also observed. The sample with an MWCNT content of 5 wt % showed a relatively low elongation at break (854%) compared to that of the NR (945%). This, to some extent, was attributed to the restriction in the molecular chain slipping along the filler surface. Therefore, the MWCNTs could carry stress throughout the NR matrix, reduce the flexibility of NR, and play a crucial role in reinforcing the nanocomposites.[30] In conclusion, NR composites containing 1–2 wt % MWCNTs possessed the highest mechanical properties. Theoretical modeling of the relationship between the morphological and mechanical properties of the NR/MWCNT composites will be investigated in the future.

CONCLUSIONS

In this study, NR/MWCNT composites were successfully prepared by a combination of the latex compounding and self-assembly techniques. The morphological structures of the composites depended on the loadings of a-MWCNTs, which were modified with PDDA as an intermedium; MWCNTs were dispersed well in NR when the loading was lower than 3 wt %, but aggregation was observed when more MWCNTs were added. These structural and morphological effects contributed directly to the thermal and mechanical properties of the composites. Significant improvements in the tensile strength and modulus was demonstrated when the MWCNT loading was between 1 and 2 wt %, whereas a further increase in the loading showed only limited reinforcement. The MWCNT dispersion in the composites could have implications for other properties, such as the electrical conductivity; this will be the focus of future research.

References

1. Almecija, D.; Blond, D.; Sader, J. E.; Coleman, J. N.; Boland, J. J. Carbon 2009, 47, 2253.
2. Warren, S. C.; Messina, L. C.; Slaughter, L. S.; Kamperman, M.; Zhou, Q.; Gruner, S. M.; DiSalvo, F. J.; Wiesner, U. Science 2008, 320, 1748.
3. Baller, J.; Becker, N.; Ziehmer, M.; Thomassey, M.; Zielinski, B.; Muller, U.; Sanctuary, R. Polymer 2009, 50, 3211.
4. Pan, L. K.; Wang, X. Z.; Gao, Y.; Zhang, Y. P.; Chen, Y. W.; Sun, Z. Desalination 2009, 244, 139.
5. Vast, L.; Carpentier, L.; Lallemand, F.; Colomer, J. F.; Van Tendeloo, G.; Fonseca, A.; Nagy, J. B.; Mekhalif, Z.; Delhalle, J. J Mater Sci 2009, 44, 3476.
6. Hirsch, A. Angew Chem Int Ed 2002, 41, 1853.
7. Rattanasom, N.; Prasertsri, S.; Suchiva, K. J Appl Polym Sci 2009, 113, 3985.

8. Shin, C. H.; Kim, D. S. Polym Adv Technol 2008, 19, 1062.
9. Ramanan, K.; Richard, A. Polymer Nanocomposites: Synthesis, Characterization, and Modeling; Oxford University Press: New York, 2001.
10. Yorifuji, D.; Matsumura, A.; Aoki, T.; Tashiro, Y.; Kuroki, S.; Ando, S. J Photopolym Sci Technol 2009, 22, 447.
11. Susteric, Z.; Kos, T. Appl Rheol 2008, 18, 54894.
12. Zhao, Y. Y.; Qiu, Z. B.; Yang, W. T. J Phys Chem B 2008, 112, 16461.
13. Peng, Z.; Kong, L. X. Polym Degrad Stab 2007, 92, 1061.
14. Peng, Z.; Kong, L. X.; Li, S. D.; Chen, Y.; Huang, M. F. Compos Sci Technol 2007, 67, 3130.
15. Zhao, X. D.; Lin, W. R.; Song, N. H.; Chen, X. F.; Fan, X. H.; Zhou, Q. F. J Mater Chem 2006, 16, 4619.
16. Bhattacharyya, S.; Sinturel, C.; Bahloul, O.; Saboungi, M. L.; Thomas, S.; Salvetat, J. P. Carbon 2008, 46, 1037.
17. Peng, Z.; Feng, C. F.; Luo, Y. Y.; Li, Y. Z.; Kong, L. X. Carbon 2010, 48, 4497.
18. Decher, G.; Hong, J. D. Makromol Chem Macromol Symp 1991, 46, 321.
19. Kotov, N. A. Nanostruct Mater 1999, 12, 789.
20. Shimazaki, Y.; Mitsuishi, M.; Ito, S.; Yamamoto, M. Langmuir 1997, 13, 1385.
21. Kim, J.; Wang, H. C.; Kumar, J.; Tripathy, S. K. Chem Mater 1999, 11, 2250.
22. Cassagneau, T.; Guérin, F.; Fendler, J. H. Langmuir 2000, 16, 7318.
23. Katagiri, K.; Caruso, F. Macromolecules 2004, 37, 9947.
24. Lvov, Y.; Ariga, K.; Onda, M.; Ichinose, I.; Kunitake, T. Langmuir 1997, 13, 6195.
25. Kueseng, K.; Jacob K, I. Eur Polym J 2006, 42, 220.
26. Kim, J. Y.; Il Han, S.; Hong, S. P. Polymer 2008, 49, 3335.
27. Yu, H. P.; Li, S. D.; Zhong, J. P.; Xu, K. Thermochim Acta 2004, 410, 119.
28. Marosi, G.; Marton, A.; Szep, A.; Csontos, I.; Keszei, S.; Zimonyi, E. Polym Degrad Stab 2003, 82, 379.
29. Peng, Z.; Kong, L. X.; Li, S. D.; Chen, Y.; Huang, M. F. Compos Sci Technol 2007, 67, 3130.
30. Sui, G.; Zhong, W. H.; Yang, X. P.; Yu, Y. H.; Zhao, S. H. Polym Adv Technol 2008, 19, 1543.